JOC The Journal of Organic Chemistry

Article

pubs.acs.org/joc

Pentaleno[1,2-*a*:4,5′]diacenaphthylenes: Uniquely Stabilized Pentalene Derivatives

Bingxin Yuan,[‡] Junpeng Zhuang,[‡] Kristopher M. Kirmess,[‡] Chelsea N. Bridgmohan,[‡] Adam C. Whalley,[†] Lichang Wang,[‡] and Kyle N. Plunkett*[,‡]

[‡]Department of Chemistry and Biochemistry and the Materials Technology Center, Southern Illinois University, Carbondale, Illinois 62901, United States

[†]Department of Chemistry, The University of Vermont, Burlington, Vermont 05405, United States

Supporting Information

ABSTRACT: We demonstrate the preparation of diacenaphthopentalene derivatives via a palladium-catalyzed dimerization of 1-iodo-2-arylethynyl-acenaphthylenes. The resulting 7,14-diarylpentaleno[1,2-*a*:4,5*a*′]diacenaphthylenes, which contain four linearly fused five-membered rings, are benchtop stable and behave as hole-transporting or ambipolar semiconductors in organic field effect transistors. The X-ray crystal structure shows the important role of the fused naphthalene unit that enforces a formal pentalene subunit at the central five-membered rings and [5]-radialene-like structures at the proximal five-membered rings. Nucleus-independent chemical shift (NICS) calculations show the internal pentalene rings are intermediate in antiaromaticity character between known pentalene and dibenzopentalenes derivatives. The diacenaphthopentalene derivatives give high optical gap materials owing to a forbidden HOMO to LUMO transition, yet have narrow electrochemical gaps and are reduced at small negative potentials giving LUMO energy levels of −3.57 to −3.74 eV.

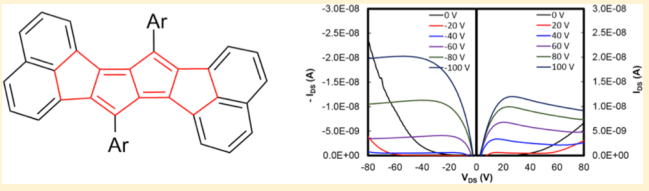

INTRODUCTION

Fully unsaturated oligoquinanes, which are multiple fused five-membered ring compounds, have been the subject of experimental and theoretical investigations to probe fundamental aromatic properties for several decades.[1] Inquiries into the linear oligoquinane analogs have arisen owing to the structural similarity to the more well-known acenes, which are composed of multiple linearly fused six-membered rings. The limiting factor for studying oligoquinanes so far is their inherent instability.[1] The smallest oligoquinane is pentalene **1** (Figure 1), a structural unit that is unstable except for sterically protected derivatives,[2] when used as a ligand for metal complexes,[3] or when annulated to other aromatic rings.[4−6] While the native pentalene is known to readily dimerize above −140 °C,[7,8] a growing list of aryl-fused pentalenes[9−24] (e.g., **2**) are known to be quite stable owing to the delocalization of the pentalene double bonds into the adjoined aromatic subunits. Many of these materials have been successfully incorporated as active components in organic field effect transistors (OFETs).[12,19,20,24] Larger oligoquinane derivatives have been studied theoretically[25−28] and are physically known, yet are very rare. Two separate groups[29−31] have reported the synthesis of tetraquinane derivatives (**3** and **4**) that employ sterically bulky groups to access structures that are fleeting in solution and in the solid state. Owing to their general instability, higher ordered oligoquinanes such as hexaquinane (**5**) have been predicted to be too unstable to be prepared.[1] Although, a tetraquinane derivative has lasted long enough to obtain an X-ray crystal structure,[31] their general instability is detrimental to investigating their utility as active components in electronic devices. With recent advances in synthetic methodologies to access pentalene derivatives, we have revisited the synthesis of multiple-fused five-membered rings that can be stabilized by annulation chemistry.

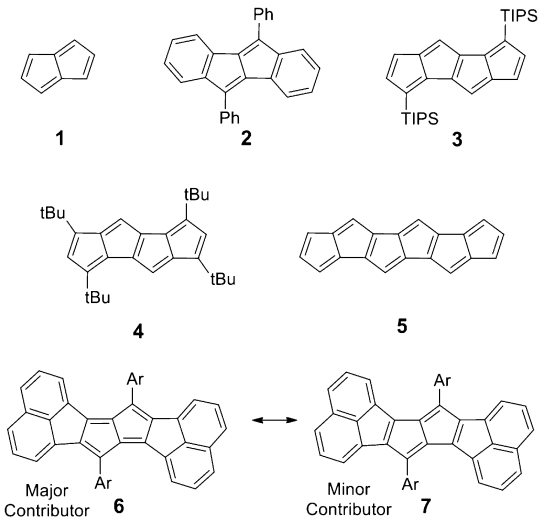

Figure 1. Oligoquinane structures.

Received: June 21, 2016
Published: August 25, 2016

DOI: 10.1021/acs.joc.6b01480
J. Org. Chem. 2016, 81, 8312−8318

Scheme 1. Synthesis of 1-Iodo-2-arylethynyl-acenaphthylenes 13a−e

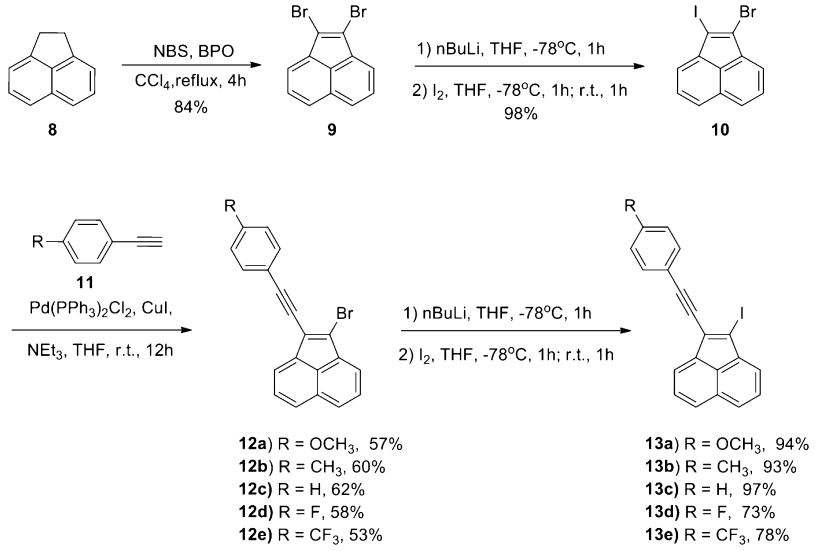

Scheme 2. Synthesis of 7,14-Diarylpentaleno[1,2-*a*:4,5*a*′]diacenaphthylenes 6a−e

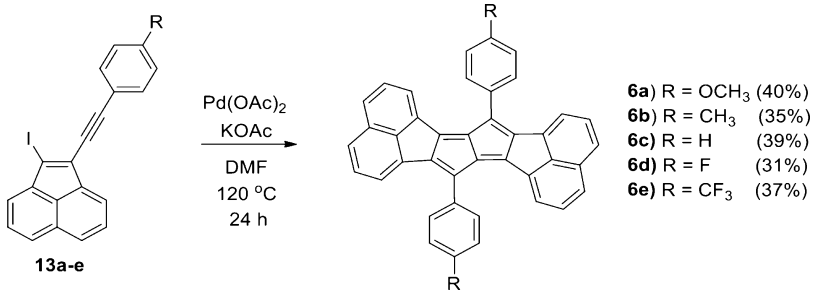

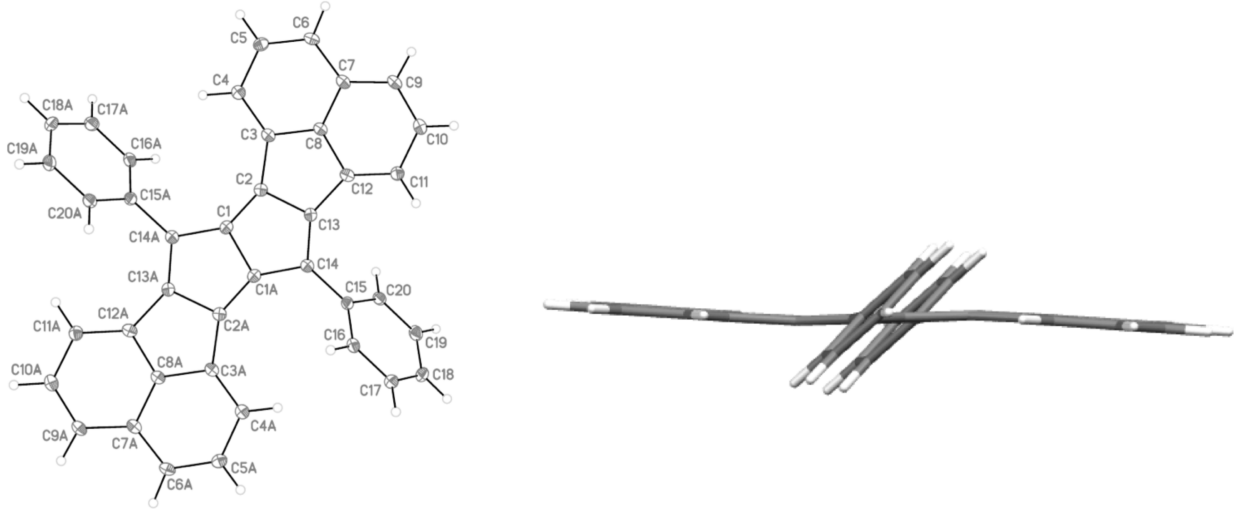

Figure 2. Molecular structure of **6c** represented as thermal ellipsoid with a 50% probability and labeled carbons (left). Side-view of **6c** showing the 6.1° offset between the inner pentalene subunit and the outer naphthalene subunits.

RESULTS AND DISCUSSION

Although the effort to synthesize the previous tetraquinanes was impressive, the methodologies employed were laborious. Recent advances in metal-catalyzed annulation transformations[32] have allowed for quick and efficient methods to access the growing library of aryl-fused pentalenes.[9−24] Currently, the most common strategy is the transition metal catalyzed dimerization of various *o*-bromoethynylbenzenes.[10,11] Owing to the simplicity of such a strategy, we chose to build new oligoquinane derivatives via a dimerization reaction of compounds that already possessed five-membered rings such as acenaphthylenes. To access such building blocks, we employed the well-known bromination[33] of acenaphthene **8** to begin a convenient synthesis (Scheme 1) of a series of 1-iodo-2-arylethynyl-acenaphthylenes **13a−e** with electron-rich as well as electron-poor para-substituents. Reaction selectivity was

DOI: 10.1021/acs.joc.6b01480
J. Org. Chem. 2016, 81, 8312−8318

enabled by desymmeterizing **8** to 1-bromo-2-iodoacenaphthylene **9** via lithiation followed by quenching with iodine. A selective Sonogashira cross-coupling between the iodo functionality and a variety of aryl-ethynylenes **11** could then be utilized to give the 1-bromo-2-arylethynyl-acenaphthylenes **12a−e**. Final transformation to access the 1-iodo-2-arylethynyl-acenaphthylenes **13a−e** was accomplished via lithiation followed by quenching with iodine. A catalyst system of $Pd(OAc)_2$ and KOAc in DMF at 120 °C was then utilized to facilitate the palladium-catalyzed dimerization/annulation of **13a−e** to give 7,14-diarylpentaleno[1,2-*a*:4,5-*a*′]diacenaphthylenes **6a−e** in reasonable yields of 31−40% (Scheme 2). As demonstrated previously,[10] the iodo-functionalized **13a−e** gave better yields for this palladium-catalyzed dimerization than the corresponding bromides **12a−e**. The resulting compounds can be formally considered pentalenes with two flanking acenaphthene groups and are red solids that are stable in the solid state and moderately stable in solution (Supporting Information).

Crystals[34] of **6c** suitable for X-ray diffraction were grown by the horizontal physical vapor transport growth technique (Figure 2).[35] In contrast to the fully planar arrangement of previous tetraquinanes,[31] the four five-membered ring sequence of **6c** does not give a completely planar arrangement. Rather, three planes are formed with the interior pentalene unit creating a single plane and each of the acenaphthylene units creating two additional planes that are bent by an angle of 6.1°. The bent nature of the molecule is directly related to the steric congestion between the naphthyl groups and the aryl rings that are appended to the five-membered rings. Detailed investigation of the carbon−carbon bond lengths (Table 1) demonstrates that resonance form **6** is more predominant than **7** giving a pentalene core and two naphthyl residues (Figure 1). This finding is significant because all currently known diarylpentalenes show bond lengths in the internal five-membered rings to be consistent with the isolation of a double bond onto an attached aryl group to give Clar sextets[36] (e.g., **2** same bonding at **7**). However, for **6c** the naphthalene moiety enforces a radialene bonding pattern (e.g., [5]-radialene[37]) at the proximal five-membered rings and a more traditional pentalene unit at the core. This assignment brings question to the aromaticity/antiaromaticity of the five-membered rings. If the pentalene is isolated electronically, it would possess eight electrons and be formally antiaromatic. Owing to the lack of protons on the five-membered rings, we are unable to use ^{1}H NMR to probe the extent of delocalization or the paratropic/diatropic properties of these compounds. However, we have performed nucleus-independent chemical shift (NICS) calculations to probe the magnetic shielding at the centers of each ring.[38−40] Owing to symmetry, **6c** possesses two chemically different five-membered rings and two chemically different six-membered rings. The innermost five-membered rings give clearly antiaromatic NICS(1) values of 11.8 ppm while the exterior five-membered rings give a nonaromatic (or slightly aromatic) chemical shift of −1.1 ppm (Table 2). Both of the exterior six-membered rings give aromatic values (−10.2 and −10.1 ppm) as expected. The harmonic oscillator model of aromaticity (HOMA)[41] values give a slightly alternative representation with both five-membered rings showing mild antiaromaticity (Supporting Information). Comparison of the NICS(1) values to **1−3** may provide a reasonable explanation for the increased stability of the 7,14-diarylpentaleno[1,2-*a*:4,5-*a*′]diacenaphthylenes synthesized here. For the known unstable compounds **1** and **3**, the highest NICS(1) values are 19.4 and 18.2 ppm, respectively, which are considerably higher than **6c**. In contrast, the well-known stabilized dibenzopentalene **2** gives a less antiaromatic value of 6.0 ppm. If one considers antiaromatic character as a defining property for stability, **6c** would lie somewhere in between these extremes.

The optical and electrochemical properties of **6a−e** were investigated with absorption spectroscopy and cyclic voltammetry. Each derivative gave identical absorption spectra (Figure 3 and Supporting Information) with small variance in the molar absorption coefficient. The λ_{max} for **6c** is 358 nm with an onset of absorption at 539 nm, which coincides with an optical gap of 2.30 eV (Table 3). These values are considerably higher than other recent planar cyclopenta-fused polycyclic aromatic hydrocarbons (CP-PAHs) that show optical gaps as low as 1.2 eV.[42−46] The compounds were not emissive (or very weakly emissive, Supporting Information), a property shared with many other planar CP-PAHs.[47,48,43,49] Solution-based cyclic voltammetry of **6a−e** demonstrated that all compounds gave pseudoreversible oxidation waves and two reversible reduction waves (Figure 4). Both the onset of oxidation as well as that of the reduction waves vary with respect to the substituents, with the oxidation occurring at less positive potentials with the more electron-rich substituents (R = OCH_3) and the reduction waves occurring at less negative potentials with the more electron-poor (R = CF_3) substituents. The highest occupied molecular orbital (HOMO) and lowest unoccupied molecular orbital

Table 1. Calculated and Experimental Bond Lengths of 6c

bond	DFT (Å)	X-ray (Å)
C1−C2	1.371	1.371
C2−C3	1.457	1.462
C3−C4	1.388	1.377
C4−C5	1.419	1.414
C5−C6	1.388	1.377
C6−C7	1.424	1.418
C7−C9	1.426	1.415
C9−C10	1.386	1.377
C10−C11	1.421	1.414
C11−C12	1.387	1.378
C12−C13	1.458	1.458
C13−C14	1.374	1.367
C14−C1A	1.475	1.471
C1−C1A	1.473	1.470
C2−C13	1.505	1.495
C3−C8	1.431	1.422
C7−C8	1.410	1.406
C8−C12	1.431	1.427

Table 2. Summary of NICS(1) Values of 1−3, 6c[a]

compd	P1	P2	H1	H2
1	19.4	–	–	–
2	6.0	–	−5.6	–
3	18.2	13.7	–	–
6c	11.8	−1.1	−10.2	−10.1

[a]P = pentacycle, H = hexacycle. P1 being more internal than P2. Explicit numbering of rings found in Supporting Information. Negative values indicate aromaticity while positive values indicate antiaromaticity.

DOI: 10.1021/acs.joc.6b01480
J. Org. Chem. 2016, 81, 8312−8318

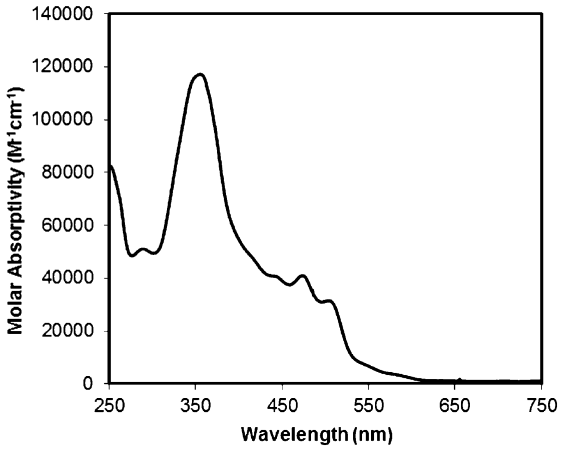

Figure 3. Representative absorption spectra of diacenaphthopentalene **6c** in chloroform.

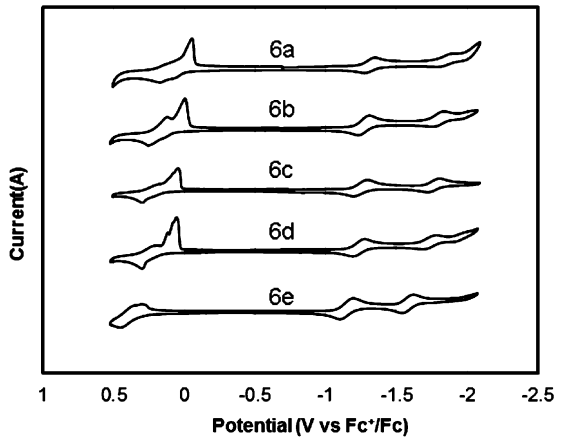

Figure 4. Cyclic voltammographs of 0.03 mM **6a**−**e** in THF with 0.1 M tetrabutyl ammonium hexafluorophosphate, glassy carbon working electrode, platinum counter electrode, and an Ag/AgCl reference electrode. Scan rate = 50 mV/s. Ferrocene added to subsequent scan as internal standard and referenced to 0 V.

(LUMO) energies were estimated by comparing to a ferrocene standard. The HOMO values varied from −4.79 to −5.07 eV, and the LUMO values varied from −3.57 to −3.74 eV (Table 3). The low lying LUMOs result from the ability to reduce the pentalene to an aromatic system. A direct comparison of the $E_{1/2}$ reductions (Supporting Information) of these compounds demonstrates they are slightly easier to reduce in relation to other recently reported aryl-fused pentalene (and multi-pentalene) containing compounds.

Comparison of the optical and electrochemical energy gaps obtained for **6a**−**e** (Table 3) highlights a dramatic discrepancy in energy values (>1 eV). In our past experiences with other planar CP-PAHs, we found smaller deviations on the order of 0.2−0.4 eV.[44,45] To elucidate the significant difference in the electronic transitions observed in **6a**−**e**, we performed density functional theory (DFT) and time-dependent DFT (TDDFT) calculations. TDDFT calculations showed that the HOMO−LUMO transition is optically forbidden (f = 0.00) for all 7,14-diarylpentaleno[1,2-*a*:4,5-*a*′]diacenaphthylenes studied here. In contrast, the experimentally observed optical gap corresponds to the HOMO−1 to LUMO transition, with no evidence of a near-IR forbidden HOMO to LUMO transition at longer wavelengths (Supporting Information). Figure 5 depicts the HOMO−1, HOMO, and LUMO contour plots of **6c** (Supporting Information for remaining compounds). The DFT calculated results showed that the HOMO−1 to LUMO transition is about 0.9 eV higher than the HOMO−LUMO transition, therefore providing an explanation for the considerable difference between the electrochemical and optical measurements.

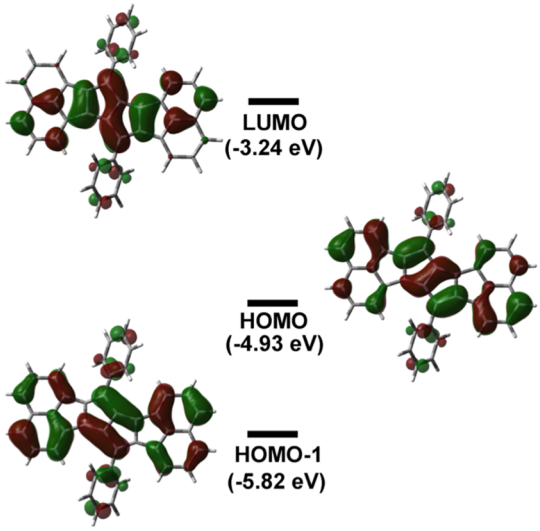

Figure 5. B3LYP/6-31+G(d,p) calculated HOMO−1, HOMO, and LUMO contours and energies of **6c**.

The crystal packing of **6c** grown from the vapor phase showed a π-stacking arrangement with significant overlap between naphthalene units on adjacent molecules, albeit in a tilted arrangement (Figure 6). To assess these materials as active components for charge transport, we fabricated OFETs in bottom-gate top-contact devices by thermal evaporation of

Table 3. Summary of Optoelectrochemical and OFET Properties of 6a−e[a]

compd	$E_{ox/onset}$ (V)	$E_{red/onset}$ (V)	HOMO (eV)	LUMO (eV)	$E_{chem\ gap}$ (eV)	optical gap (eV)	mobility[b] ($cm^2\ V^{-1}\ s^{-1}$)
6a	−0.015	−1.23	−4.79	−3.57	1.22	2.29	1.7×10^{-4}
6b	0.067	−1.19	−4.87	−3.61	1.26	2.28	2.3×10^{-3}
6c	0.12	−1.17	−4.92	−3.63	1.29	2.30	4.0×10^{-4}
6d	0.14	−1.16	−4.94	−3.64	1.30	2.34	5.4×10^{-4}
6e	0.27	−1.06	−5.07	−3.74	1.33	2.34	3.2×10^{-4} (5.8×10^{-5})[c]

[a]Measurements taken at sample concentration of 0.03 mM and potentials measured relative to a ferrocenium/ferrocene redox couple used as an internal standard with a glassy carbon working electron, platinum counter electrode and Ag/AgCl reference electrode (Figure 4). $E_{ox/onset}$ is the onset of oxidation potential; $E_{red/onset}$ is the onset of reduction potential. HOMO and LUMO values calculated on the basis of the oxidation of the ferrocene reference in vacuum (4.8 eV). [b]Hole mobilities with average of at least three channels. [c]Electron mobility of **6e**.

DOI: 10.1021/acs.joc.6b01480
J. Org. Chem. 2016, 81, 8312−8318

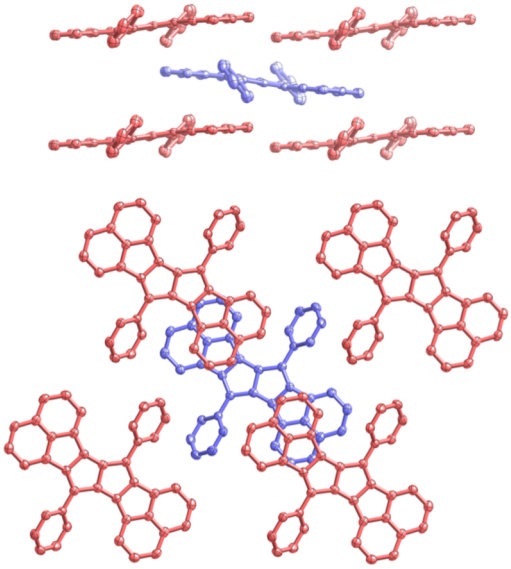

Figure 6. Side view (top) and top view (bottom) of the crystal packing of **6c**.[34]

6a–e onto octadecyltrichlorosilane (OTS) functionalized Si/SiO_2 followed by deposition of gold contacts (Supporting Information). We found the OFETs measured in air with a negative gate voltage operated in the hole-transporting regime with charge carrier mobilities on the order of 10^{-4} to 10^{-3} cm^2 V^{-1} s^{-1} (Table 3). When performing measurement in an argon filled glovebox, **6e** alone gave ambipolar charge transport[24] characteristics with hole mobility of 3.2×10^{-4} and electron mobility of 5.8×10^{-5} cm^2 V^{-1} s^{-1}, respectively (Figures 7 and 8). The described values are not exceedingly high and could be a result of nonoptimal π-stacking in the solid state from the thermal evaporation.

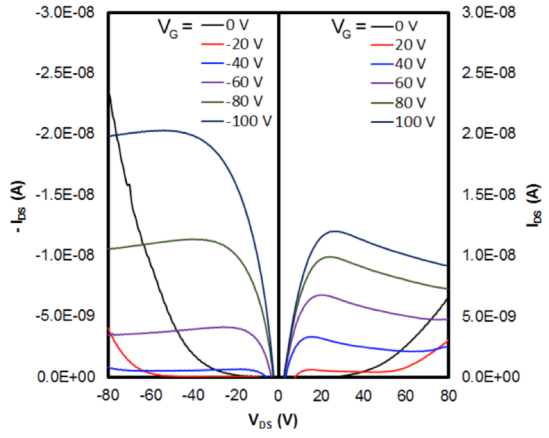

Figure 7. Typical output curve for **6e** showing ambipolar behavior.

In conclusion, we have utilized a simple, palladium-catalyzed dimerization of 1-iodo-2-arylethynyl-acenaphthylenes to access oligoquinanes with electronically isolated pentalene motifs. Owing to the unique annulation of naphthalene units, the central five-membered rings show bonding lengths that are more pentalene-like than other diarylpentalenes. The 7,14-diarylpentaleno[1,2-*a*:4,5-*a*′]diacenaphthylenes **6a–e** give large optical band gaps, owing to the lack of HOMO to LUMO transition, but still offer a reduced electrochemical gap with

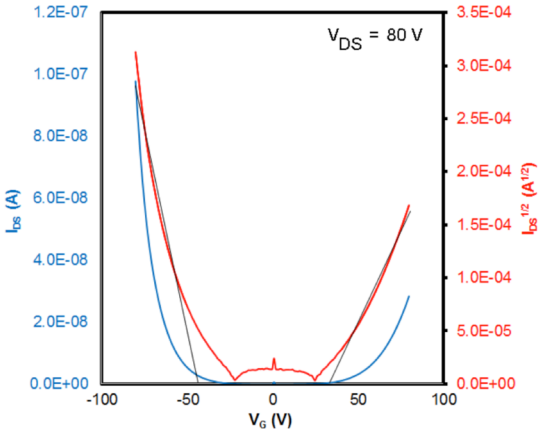

Figure 8. Typical transfer plot for ambipolar **6e** ($h^+ = 3.2 \times 10^{-4}$ cm^2 V^{-1} s^{-1}, $e^- = 5.8 \times 10^{-5}$ cm^2 V^{-1} s^{-1}).

LUMO levels as low as −3.74 eV. The annulation strategy described here may offer a key route to access higher ordered oligoquinanes, a topic we are currently pursuing.

EXPERIMENTAL SECTION

General Procedures. Unless otherwise noted, all reagents were used as received and all reactions were carried out under an argon atmosphere. ^{1}H NMR and ^{13}C NMR were recorded on a 400 MHz NMR station at room temperature, unless otherwise noted. Cyclic voltammetry was performed with a 0.1 M tetrabutyl-ammonium hexafluorophosphate solution (THF) using a glassy carbon electrode, platinum counter electrode, and a Ag/AgCl reference electrode.

*1,2-Dibromoacenaphthylene (**9**):*[33] A CCl_4 solution (250 mL) of acenaphthene **8** (15.4 g, 100.0 mmol), *N*-bromosuccinimide (53.4 g, 300.0 mmol), and benzoyl peroxide (2.43 g, 10.0 mmol) was heated to reflux for 4 h. The cooled reaction mixture was filtered to remove the solid byproduct. The filtrate was collected and then extracted with 1 M $NaHSO_3$, water, and brine. The organic phase was dried with anhydrous $MgSO_4$. After removal of the solvent in vacuo, the residue was recrystallized in ethanol to give 26.1 g (84%) of a yellow solid: ^{1}H NMR (400 MHz, $CDCl_3$) δ 7.84 (d, J = 8.2 Hz, 2H), 7.66 (d, J = 6.7 Hz, 2H), 7.57 (dd, J = 8.2, 7.0 Hz, 2H). ^{13}C NMR (100 MHz, $CDCl_3$) δ 136.8, 128.1, 127.8, 127.2, 126.5, 123.1, 121.0.

*1-Bromo-2-iodoacenaphthylene (**10**).* To a solution of **9** (14.0 g, 39.0 mmol) in THF (200 mL) was added *n*BuLi (1.6 M in hexane, 31 mL, 54 mmol) at −78 °C. The mixture was stirred for 1 h, and I_2 (13.5 g, 87.8 mmol) in 25 mL THF was added slowly. The mixture was stirred at rt under argon for 1 h, poured into 1 M $NaHSO_3$, and extracted with dichloromethane. The organic layer was washed with water and brine and dried over anhydrous $MgSO_4$. The solvent was removed in vacuo to give 16.1 g (98%) of an orange solid, mp = 77–79 °C: ^{1}H NMR (400 MHz, $CDCl_3$) δ 7.97 (dd, J = 8.1, 0.7 Hz, 2H), 7.75 (d, J = 7.4 Hz, 1H), 7.65–7.58 (m, 2H), 7.43 (d, J = 7.4 Hz, 1H). ^{13}C NMR (100 MHz, $CDCl_3$) δ 137.1, 136.4, 130.9, 128.8, 127.4, 127.3, 127.2, 124.1, 123.7, 123.5, 120.9, 120.7. LRMS (EI+) 355.9 HRMS: m/z for $C_{12}H_6BrI$ calcd 355.8698, found 355.8704.

*General Procedure for 1-Bromo-2-arylethynyl-acenaphthylene Derivatives (**12a–e**).* In a glovebox, **10** (5.60 mmol), a corresponding arylethynylene **11** (5.60 mmol), $PdCl_2(PPh_3)_2$ (197 mg, 0.28 mmol), CuI (54 mg, 0.28 mmol), triethylamine (10 mL), and THF (10 mL) were combined in a round-bottom flask and stirred at rt for 6 h. The reaction mixture was passed over Celite and washed with hexane. The solvent was removed in vacuo, and the residue was purified by column chromatography on silica gel.

*1-Bromo-2-((4-methoxyphenyl)ethynyl)acenaphthylene (**12a**).* (Column and TLC with 40% CH_2Cl_2 in hexane, R_f = 0.3) orange solid, isolated yield 57% (1.15 g), mp = 101–103 °C; ^{1}H NMR (400 MHz, $CDCl_3$) δ 7.88 (d, J = 8.1 Hz, 1H), 7.85–7.77 (m, 2H), 7.69 (d, J = 6.8 Hz, 1H), 7.64–7.52 (m, 4H), 6.93 (d, J = 8.1 Hz, 2H), 3.86 (s,

DOI: 10.1021/acs.joc.6b01480
J. Org. Chem. 2016, 81, 8312–8318

3H). ^{13}C NMR (100 MHz, $CDCl_3$) δ 160.0, 138.0, 137.7, 133.4, 128.8, 128.1, 128.0, 127.7, 127.6, 127.0, 123.6, 123.6, 123.6, 122.9, 115.3, 114.1, 100.2, 82.4, 55.4. LRMS (EI+): 361.2; HRMS: m/z for $C_{21}H_{13}BrO$ calcd 360.0150, found 360.0172.

*1-Bromo-2-(p-tolylethynyl)acenaphthylene (**12b**).* (Column and TLC with 10% CH_2Cl_2 in hexane, R_f = 0.3) orange solid, isolated yield 60% (1.16 g), mp = 102−104 °C; ^{1}H NMR (400 MHz, $CDCl_3$) δ 7.89 (dd, J = 8.8, 5.6 Hz, 1H), 7.86−7.81 (m, 2H), 7.69 (t, J = 7.2 Hz, 1H), 7.64−7.53 (m, 4H), 7.21 (d, J = 8.1 Hz, 2H), 2.40 (s, 3H). ^{13}C NMR (100 MHz, $CDCl_3$) δ 139.0, 138.0, 137.7, 131.8, 129.3, 128.9, 128.1, 128.1, 127.7, 127.7, 127.0, 124.0, 123.7, 123.6, 123.0, 120.1, 100.3, 82.9, 21.7. LRMS (EI+): 344.1; HRMS: m/z for $C_{21}H_{13}Br$ calcd 344.0201, found 344.0189.

*1-Bromo-2-(phenylethynyl)acenaphthylene (**12c**).* (Column and TLC with 10% CH_2Cl_2 in hexane, R_f = 0.3) orange solid, isolated yield 62% (1.15 g), mp = 107−110 °C; ^{1}H NMR (400 MHz, $CDCl_3$) δ 7.90 (d, J = 8.1 Hz, 1H), 7.85 (dd, J = 7.6, 4.0 Hz, 2H), 7.72 (d, J = 6.9 Hz, 1H), 7.69−7.64 (m, 2H), 7.64−7.57 (m, 2H), 7.45−7.37 (m, 3H). ^{13}C NMR (100 MHz, $CDCl_3$) δ 137.9, 137.6, 131.8, 129.0, 128.7, 128.5, 128.1, 128.1, 127.7, 127.7, 127.0, 124.5, 123.8, 123.3, 123.2, 123.0, 99.9, 83.5. LRMS (EI+): 330.0; HRMS: m/z for $C_{20}H_{11}Br$ calcd 330.0044, found 330.0052.

*1-Bromo-2-((4-fluorophenyl)ethynyl)acenaphthylene (**12d**).* (Column and TLC with 10% CH_2Cl_2 in hexane, R_f = 0.3) orange solid, isolated yield 58% (1.13 g), mp = 74−76 °C; ^{1}H NMR (400 MHz, $CDCl_3$) δ 7.89 (t, J = 6.9 Hz, 1H), 7.84 (dd, J = 7.5, 4.5 Hz, 2H), 7.71 (d, J = 6.9 Hz, 1H), 7.66−7.57 (m, 4H), 7.13−7.07 (m, 2H). ^{13}C NMR (100 MHz, $CDCl_3$) δ 162.8 (d, $^1J_{C-F}$ = 246.3 Hz), 137.8, 137.5, 133.9 (d, $^3J_{C-F}$ = 8.75 Hz), 133.8, 129.1, 128.1, 128.1, 127.7, 127.0, 124.6, 123.9, 123.2, 123.0, 119.4, 119.4, 115.8 (d, $^2J_{C-F}$ = 22.5 Hz), 98.8, 83.3. LRMS (EI+): 349.2; HRMS: m/z for $C_{20}H_{10}BrF$ calcd 347.9950, found 347.9974.

*1-Bromo-2-((4-(trifluoromethyl)phenyl)ethynyl)acenaphthylene (**12e**).* (Column and TLC with 10% CH_2Cl_2 in hexane, R_f = 0.3) orange solid, isolated yield 53% (1.18 g), mp = 158−160 °C; ^{1}H NMR (400 MHz, $CDCl_3$) δ 7.93 (d, J = 8.1 Hz, 1H), 7.86 (dd, J = 7.5, 4.1 Hz, 2H), 7.75 (dd, J = 7.7, 3.7 Hz, 3H), 7.68−7.58 (m, 4H); ^{13}C NMR (100 MHz, $CDCl_3$) δ 137.6, 137.3, 131.9, 130.2 (q, $^2J_{C-F}$ = 32.3 Hz), 129.4, 128.1, 128.1, 127.8, 127.8, 126.9, 125.7, 125.3 (q, $^3J_{C-F}$ = 3.7 Hz), 124.8 (q, $^1J_{C-F}$ = 213.0 Hz), 124.2, 123.0, 122.6, 98.1, 85.8. LRMS (EI+): 398.0; HRMS: m/z for $C_{21}H_{10}BrF_3$ calcd 397.9918, found 397.9911.

*General Procedure for 1-Iodo-2-arylethynyl-acenaphthylene Derivatives (**13a**−**e**).* To a solution of **12a**−**e** (2.42 mmol) in THF (20 mL) was added *n*BuLi (1.6 M in hexane, 1.6 mL, 2.47 mmol) at −78 °C. The mixture was stirred for 1 h, and I_2 (0.63 g, 2.25 mmol) in 4 mL THF was added slowly. The mixture was stirred at rt under argon for 1 h, poured into 1 M $Na_2S_2O_3$, and extracted with dichloromethane. The organic layer was washed with distilled water and brine and dried with anhydrous $MgSO_4$. The solvent was removed in vacuo, and the residue was carried on to the next step without further purification.

*1-Iodo-2-((4-methoxyphenyl)ethynyl)acenaphthylene (**13a**).* Orange solid, isolated yield 94%; ^{1}H NMR (400 MHz, $CDCl_3$) δ 7.89−7.83 (m, 2H), 7.81 (d, J = 8.2 Hz, 1H), 7.63−7.58 (m, 3H), 7.58−7.49 (m, 2H), 6.93 (d, J = 8.9 Hz, 2H), 3.86 (s, 3H). ^{13}C NMR (100 MHz, $CDCl_3$) δ 160.1, 140.6, 139.2, 133.4, 130.3, 128.6, 128.1, 128.1, 128.0, 127.8, 127.4, 125.4, 122.7, 115.4, 114.2, 100.2, 97.3, 84.5, 55.4. LRMS (EI+): 408.0; HRMS: m/z for $C_{21}H_{13}IO$ calcd 408.0011, found 408.0012.

*1-Iodo-2-(p-tolylethynyl)acenaphthylene (**13b**).* Orange solid, isolated yield 93%; ^{1}H NMR (400 MHz, $CDCl_3$) δ 7.91 (dd, J = 14.4, 6.4 Hz, 2H), 7.84 (d, J = 8.3 Hz, 1H), 7.65 (dd, J = 8.1, 7.0 Hz, 1H), 7.60 (m, 4H), 7.24 (d, J = 7.9 Hz, 2H), 2.43 (s, 3H); ^{13}C NMR (100 MHz, $CDCl_3$) δ 140.5, 139.2, 139.0, 131.8, 130.2, 129.3, 128.8, 128.1, 128.0, 127.8, 127.5, 125.5, 122.8, 120.2, 100.3, 97.8, 85.1, 21.7. LRMS (EI+): 392.1. HRMS: m/z for $C_{21}H_{13}I$ calcd 392.0062, found 392.0069.

*1-Iodo-2-(phenylethynyl)acenaphthylene (**13c**).* Orange solid, isolated yield 97% (0.96 g); ^{1}H NMR (400 MHz, $CDCl_3$) δ 7.91−7.84 (m, 2H), 7.84−7.78 (m, 1H), 7.71−7.65 (m, 2H), 7.65−7.54 (m, 3H), 7.44−7.37 (m, 3H). ^{13}C NMR (100 MHz, $CDCl_3$) δ 139.2, 139.2, 131.9, 131.8, 129.0, 128.8, 128.6, 128.2, 127.6, 125.7, 123.3, 122.9, 122.9, 122.8, 100.0, 98.4. LRMS (EI+): 378.2. HRMS: m/z for $C_{20}H_{11}I$ calcd 378.9905, found 378.9918.

*1-((4-Fluorophenyl)ethynyl)-2-iodoacenaphthylene (**13d**).* Orange solid, isolated yield 73%; ^{1}H NMR (400 MHz, $CDCl_3$) δ 7.97−7.88 (m, 1H), 7.84 (dd, J = 7.5, 4.1 Hz, 2H), 7.72 (d, J = 7.0 Hz, 1H), 7.69−7.57 (m, 5H), 7.09 (m, 2H). ^{13}C NMR (100 MHz, $CDCl_3$) δ 162.8 (d, $^1J_{C-F}$ = 247.5 Hz), 137.9, 137.5, 133.8 (d, $^3J_{C-F}$ = 8.8 Hz), 129.1, 128.9, 128.1, 128.1, 128.0, 127.7, 127.6, 125.7, 123.9, 123.0, 122.8, 115.8 (d, $^2J_{C-F}$ = 21.3 Hz), 98.8, 83.3. LRMS (EI+): 396.0; HRMS: m/z for $C_{20}H_{10}FI$ calcd 395.9811, found 395.9802.

*1-Iodo-2-((4-(trifluoromethyl)phenyl)ethynyl)acenaphthylene (**13e**).* Orange solid, isolated yield 78%; ^{1}H NMR (400 MHz, $CDCl_3$) δ 7.92 (t, J = 6.5 Hz, 1H), 7.86 (m, 2H), 7.81−7.74 (m, 2H), 7.62 (m, 5H). ^{13}C NMR (100 MHz, $CDCl_3$) δ 143.9, 136.7, 131.8, 130.1 (q, ^2J_C = 32.5 Hz), 129.6, 127.9, 127.7, 127.0, 126.6, 125.4 (q, $^3J_{C-F}$ = 3.75 Hz), 125.2 (q, ^1J_C = 258.7 Hz), 124.5, 124.3, 122.7, 98.0, 86.4. LRMS (EI+): 446.2; HRMS: m/z for $C_{21}H_{10}F_3I$ calcd 445.9779, found 445.9759.

*General Procedure for 7,14-Diarylpentaleno[1,2-a:4,5-a′]-diacenaphthylenes (**6a**−**e**).* In a glovebox, **13a**−**e** (1.21 mmol), $Pd(OAc)_2$ (0.055 mmol), KOAc (1.21 mmol), and DMF (0.05M) were combined in a sealed tube and stirred for 1 day at 120 °C. The reaction mixture was cooled to room temperature and filtered. The solid was washed with H_2O and recrystallized from toluene. After recrystallization, the solid was dissolved in a large amount of hot toluene and flashed through a silica gel plug and washed with hot toluene. Due to their low solubility at room temperature, no ^{13}C NMR spectra were attainable.

*7,14-Bis(4-methoxyphenyl)pentaleno[1,2-a:4,5-a′]diacenaphthylene (**6a**).* Brown solid, isolated yield 40% (57 mg), mp = 330−332 °C; ^{1}H NMR (500 MHz, $CDCl_3$, 55 °C) δ 7.70 (t, J = 8.5 Hz, 6H), 7.57 (m, 4H), 7.40 (m, 4H), 7.22 (d, J = 7.7 Hz, 2H), 7.10 (d, J = 8.7 Hz, 4H), 3.96 (s, 6H). LRMS (EI+) 562.2; HRMS: m/z for $C_{42}H_{26}O_2$ calcd 562.1933, found 562.1924. Elemental analysis: Anal. Calcd for $C_{42}H_{26}O_2$: C, 89.66; H, 4.66. Found: C, 89.75; H, 4.52.

*7,14-Di-p-tolylpentaleno[1,2-a:4,5-a′]diacenaphthylene (**6b**).* Brown solid, isolated yield 35% (56 mg), mp = 318−320 °C; ^{1}H NMR (500 MHz, $C_6D_4Cl_2$, 120 °C) δ 7.65 (d, J = 7.9 Hz, 4H), 7.52 (d, J = 7.1 Hz, 2H), 7.46 (d, J = 7.6 Hz, 2H), 7.39 (d, J = 8.1 Hz, 2H), 7.26−7.18 (m, 10H), 2.29 (s, 6H). LRMS (EI+) 530.2; HRMS: m/z for $C_{42}H_{26}$ calcd 530.2035, found 530.2031. Elemental analysis: Anal. Calcd for $C_{42}H_{26}$: C, 95.06; H, 4.94. Found: C, 95.01; H, 4.89.

*7,14-Diphenylpentaleno[1,2-a:4,5-a′]diacenaphthylene(**6c**).* Brown solid, isolated yield 39% (59 mg), mp = 368−370 °C; ^{1}H NMR (500 MHz, $CDCl_3$, 55 °C) δ 7.78 (d, J = 8.0 Hz, 4H), 7.70 (d, J = 8.1 Hz, 2H), 7.62 (d, J = 8.1 Hz, 2H), 7.57 (m, 6H), 7.48 (d, J = 7.3 Hz, 2H), 7.44−7.36 (m, 4H), 7.17 (d, J = 7.3 Hz, 2H). LRMS (EI+) 502.1; HRMS: m/z for $C_{40}H_{22}$ calcd 502.1722, found 502.1707. Elemental analysis: Anal. Calcd for $C_{40}H_{22}$: C, 95.59; H, 4.41. Found: C, 95.48; H, 4.33.

*7,14-Bis(4-fluorophenyl)pentaleno[1,2-a:4,5-a′]diacenaphthylene (**6d**).* Brown solid, isolated yield 31% (50 mg), mp = 378−380 °C; ^{1}H NMR (500 MHz, $C_2D_2Cl_4$, 120 °C) δ 7.78 (m, 6H), 7.67 (d, 2H), 7.53 (d, 2H), 7.46 (dd, J = 6.9 Hz, 4H), 7.31 (t, 4H), 7.15 (d, 2H). LRMS (EI+) 538.1; HRMS: m/z for $C_{40}H_{20}F_2$ calcd 538.1533, found 538.1535. Elemental analysis: Anal. Calcd for $C_{40}H_{20}F_2$: C, 89.20; H, 3.74. Found: C, 89.65; H, 3.51.

*7,14-Bis(4-(trifluoromethyl)phenyl)pentaleno[1,2-a:4,5-a′]-diacenaphthylene (**6e**).* Black solid, isolated yield 37% (76 mg), mp = 371−373 °C; ^{1}H NMR (500 MHz, $C_2D_2Cl_4$, 120 °C) δ 7.88 (dd, J = 17.7, 8.1 Hz, 8H), 7.78 (d, J = 8.3 Hz, 2H), 7.71 (d, J = 8.5 Hz, 2H), 7.58 (d, J = 7.4 Hz, 2H), 7.48 (m, 4H), 7.11 (d, J = 7.5 Hz, 2H). LRMS (EI+) 638.1; HRMS: m/z for $C_{42}H_{20}F_6$ calcd 638.1469, found 638.1462. Elemental analysis: Anal. calcd for $C_{42}H_{20}F_6$: C, 78.99; H, 3.16. Found: C, 79.08; H, 3.07.

General Procedures for OFET Fabrication. OFET devices were prepared in a top contact, bottom gate configuration on a Si/SiO_2

DOI: 10.1021/acs.joc.6b01480
J. Org. Chem. 2016, 81, 8312−8318

wafer. Specifically, silicon wafers with a 300 nm oxide layer were immersed in a Piranha solution for 30 min at 50 °C, washed with DI water, and dried. The cleaned wafers were immersed in a 0.2 wt % octadecyltrichlorosilane (OTS) in toluene solution for 20 min, dunk rinsed in toluene with sonication, rinsed with toluene, and then dried. Active layers of **6a**−**e** (20 nm) were prepared by thermal evaporation through a deposition mask (Ossila, E307) at a pressure of ∼3 × 10^{-6} Torr. Source and drain electrodes were prepared by evaporating gold (50 nm) through a deposition mask (Ossila, E291) at a pressure of ∼3 × 10^{-6} Torr. Channel widths were 30 μm and channel lengths were 1 mm. Current−voltage measurements were performed on a semiconductor characterization system in air or in an argon filled glovebox.

■ ASSOCIATED CONTENT

Supporting Information

The Supporting Information is available free of charge on the ACS Publications website at DOI: 10.1021/acs.joc.6b01480.

^{1}H and ^{13}C NMR, electrochemical comparisons, computational details including atom coordinates, quantum yield, OFET fabrication, experimental and calculated UV−vis spectra (PDF)

Crystallographic data for **6c** (CIF)

■ AUTHOR INFORMATION

Corresponding Author

*E-mail: kplunkett@chem.siu.edu.

Notes

The authors declare no competing financial interest.

■ ACKNOWLEDGMENTS

This work was supported by a National Science Foundation CAREER Grant (NSF-1352431).

■ REFERENCES

(1) Haag, R.; de Meijere, A. Unsaturated Oligoquinanes and Related Systems. In *Carbon Rich Compounds I*; de Meijere, A., Ed.; Springer-Verlag: Heidelberg, 1998; pp 137−165.

(2) Hafner, K.; Süss, H. U. *Angew. Chem., Int. Ed. Engl.* **1973**, *12*, 575−577.

(3) Summerscales, O. T.; Cloke, F. G. N. *Coord. Chem. Rev.* **2006**, *250*, 1122−1140.

(4) Brand, K. *Ber. Dtsch. Chem. Ges.* **1912**, *45*, 3071−3077.

(5) Saito, M. *Symmetry* **2010**, *2*, 950−969.

(6) Hopf, H. *Angew. Chem., Int. Ed.* **2013**, *52*, 12224−12226.

(7) De Mayo, P.; Bloch, R.; Marty, R. A. *J. Am. Chem. Soc.* **1971**, *93*, 3071−3072.

(8) Bally, T.; Chai, S.; Neuenschwander, M.; Zhu, Z. *J. Am. Chem. Soc.* **1997**, *119* (8), 1869−1875.

(9) Saito, M.; Nakamura, M.; Tajima, T. *Chem. - Eur. J.* **2008**, *14*, 6062−6068.

(10) Levi, Z. U.; Tilley, T. D. *J. Am. Chem. Soc.* **2009**, *131* (8), 2796−2797.

(11) Kawase, T.; Konishi, A.; Hirao, Y.; Matsumoto, K.; Kurata, H.; Kubo, T. *Chem. - Eur. J.* **2009**, *15*, 2653−2661.

(12) Kawase, T.; Fujiwara, T.; Kitamura, C.; Konishi, A.; Hirao, Y.; Matsumoto, K.; Kurata, H.; Kubo, T.; Shinamura, S.; Mori, H.; Miyazaki, E.; Takimiya, K. *Angew. Chem., Int. Ed.* **2010**, *49*, 7728−7732.

(13) Levi, Z. U.; Tilley, T. D. *J. Am. Chem. Soc.* **2010**, *132*, 11012−11014.

(14) Yin, X.; Li, Y.; Zhu, Y.; Kan, Y.; Li, Y.; Zhu, D. *Org. Lett.* **2011**, *13*, 1520−1523.

(15) Rivera-Fuentes, P.; Rekowski, M.; von, W.; Schweizer, W. B.; Gisselbrecht, J.-P.; Boudon, C.; Diederich, F. *Org. Lett.* **2012**, *14*, 4066−4069.

(16) Maekawa, T.; Segawa, Y.; Itami, K. *Chem. Sci.* **2013**, *4*, 2369−2373.

(17) Zhao, J.; Oniwa, K.; Asao, N.; Yamamoto, Y.; Jin, T. *J. Am. Chem. Soc.* **2013**, *135*, 10222−10225.

(18) Nakano, M.; Osaka, I.; Takimiya, K.; Koganezawa, T. *J. Mater. Chem. C* **2014**, *2*, 64−70.

(19) Dai, G.; Chang, J.; Zhang, W.; Bai, S.; Huang, K.-W.; Xu, J.; Chi, C. *Chem. Commun.* **2015**, *51*, 503−506.

(20) Dai, G.; Chang, J.; Shi, X.; Zhang, W.; Zheng, B.; Huang, K.-W.; Chi, C. *Chem. - Eur. J.* **2015**, *21*, 2019−2028.

(21) Shen, J.; Yuan, D.; Qiao, Y.; Shen, X.; Zhang, Z.; Zhong, Y.; Yi, Y.; Zhu, X. *Org. Lett.* **2014**, *16*, 4924−4927.

(22) London, G.; Rekowski, M.; von, W.; Dumele, O.; Schweizer, W. B.; Gisselbrecht, J.-P.; Boudon, C.; Diederich, F. *Chem. Sci.* **2014**, *5*, 965−972.

(23) Cao, J.; London, G.; Dumele, O.; von Wantoch Rekowski, M.; Trapp, N.; Ruhlmann, L.; Boudon, C.; Stanger, A.; Diederich, F. *J. Am. Chem. Soc.* **2015**, *137*, 7178−7188.

(24) Nakano, M.; Osaka, I.; Takimiya, K. *J. Mater. Chem. C* **2015**, *3*, 283−290.

(25) Hess, B. A.; Schaad, L. J. *J. Org. Chem.* **1971**, *36*, 3418−3423.

(26) Toyota, A.; Nakajima, T. *Tetrahedron* **1981**, *37*, 2575−2579.

(27) Zhou, Z.; Parr, R. G. *J. Am. Chem. Soc.* **1989**, *111*, 7371−7379.

(28) Liu, Y.-C.; Wu, S.-X.; Su, Z.-M.; Zhang, H.-Y. *New J. Chem.* **2014**, *38*, 1092−1099.

(29) Stowasser, B.; Hafner, K. *Angew. Chem., Int. Ed. Engl.* **1986**, *25*, 466−468.

(30) Cao, H.; Flippen-Anderson, J.; Cook, J. M. *J. Am. Chem. Soc.* **2003**, *125*, 3230−3231.

(31) Cao, H.; Van Ornum, S. G.; Deschamps, J.; Flippen-Anderson, J.; Laib, F.; Cook, J. M. *J. Am. Chem. Soc.* **2005**, *127*, 933−943.

(32) Jin, T.; Zhao, J.; Asao, N.; Yamamoto, Y. *Chem. - Eur. J.* **2014**, *20*, 3554−3576.

(33) Trost, B. M.; Brittelli, D. R. *J. Org. Chem.* **1967**, *32*, 2620−2621.

(34) CCDC 1438969 (**6c**) contains the supplementary crystallographic data for this paper. These data are provided free of charge by The Cambridge Crystallographic Data Centre.

(35) Laudise, R. A.; Kloc, C.; Simpkins, P. G.; Siegrist, T. *J. Cryst. Growth* **1998**, *187*, 449−454.

(36) Clar, E. *The Aromatic Sextet*; Wiley: New York, NY, 1972.

(37) Mackay, E. G.; Newton, C. G.; Toombs-Ruane, H.; Lindeboom, E. J.; Fallon, T.; Willis, A. C.; Paddon-Row, M. N.; Sherburn, M. S. *J. Am. Chem. Soc.* **2015**, *137*, 14653−14659.

(38) Schleyer, P.; von, R.; Maerker, C.; Dransfeld, A.; Jiao, H.; Hommes, N. J. R.; van, E. *J. Am. Chem. Soc.* **1996**, *118*, 6317−6318.

(39) Chen, Z.; Wannere, C. S.; Corminboeuf, C.; Puchta, R.; Schleyer, P.; von, R. *Chem. Rev.* **2005**, *105*, 3842−3888.

(40) Stanger, A. *J. Org. Chem.* **2006**, *71*, 883−893.

(41) Kruszewski, J.; Krygowski, T. M. *Tetrahedron Lett.* **1972**, *13*, 3839−3842.

(42) Xia, H.; Liu, D.; Xu, X.; Miao, Q. *Chem. Commun.* **2013**, *49*, 4301−4303.

(43) Rose, B. D.; Shoer, L. E.; Wasielewski, M. R.; Haley, M. M. *Chem. Phys. Lett.* **2014**, *616*−*617*, 137−141.

(44) Wood, J. D.; Jellison, J. L.; Finke, A. D.; Wang, L.; Plunkett, K. N. *J. Am. Chem. Soc.* **2012**, *134*, 15783−15789.

(45) Bheemireddy, S. R.; Ubaldo, P. C.; Rose, P. W.; Finke, A. D.; Zhuang, J.; Wang, L.; Plunkett, K. N. *Angew. Chem., Int. Ed.* **2015**, *54*, 15762−15766.

(46) Frederickson, C. K.; Haley, M. M. *J. Org. Chem.* **2014**, *79*, 11241−11245.

(47) Sun, Y. P.; Wang, P.; Hamilton, N. B. *J. Am. Chem. Soc.* **1993**, *115*, 6378−6381.

(48) Bearpark, M. J.; Celani, P.; Jolibois, F.; Olivucci, M.; Robb, M. A.; Bernardi, F. *Mol. Phys.* **1999**, *96*, 645−652.

(49) Rudebusch, G. E.; Haley, M. M. Planar Cyclopenta-Fused Polycyclic Arenes; In *Polycyclic Arenes and Heteroarenes*; Miao, Q., Ed.; Wiley-VCH Verlag GmbH & Co.: 2015.

DOI: 10.1021/acs.joc.6b01480
J. Org. Chem. 2016, 81, 8312−8318